Electroless Addition of Catalytic Pd to SnO_2 Nanopowders

R. Díaz,*,† J. Arbiol,‡ A. Cirera,‡ F. Sanz,† F. Peiró,‡ A. Cornet,‡ and J. R. Morante‡

Department of Physical Chemistry, and Enginyeria i Materials Electrònics, Department of Electronics, University of Barcelona, Martí i Franqués, 1, Barcelona 08028, Spain

Received May 23, 2001. Revised Manuscript Received August 13, 2001

A new procedure based on the electroless reduction of $PdCl_2$ using Sn(II) as reducing agent is reported to efficiently add a controlled amount of Pd to nanoscaled SnO_2 powders. The characterization of these powders using XRD, Raman spectroscopy, XPS, ICP, and TEM is presented and discussed in order to show the feasibility of the proposed catalyst addition mechanism as a useful tool for the improvement of existing catalytic materials for gas sensors. Several palladium salt concentrations and reducing agent ratios and also different annealing temperatures have been used to analyze the influence on the morphology and composition of the samples. Results showed the presence of uniformly distributed metallic Pd clusters on the SnO_2 surface at any annealing temperature and the formation of well-distributed PdO clusters of less than 3 nm after annealing at sufficiently high temperature, with incorporation in this case of palladium into the nanoscaled SnO_2 particles.

Introduction

Since Seiyama et al.[1] developed the first chemical gas sensor, sensing materials that exhibit changes of conductivity after gas exposures have become a wide topic of experimental studies. Nowadays tin(IV) oxide (SnO_2) is the most used material in this kind of sensor.[2,3] Effort has been devoted to overcome most of the problems that these sensors present—mainly low sensitivity, low selectivity, and low stability. So it has been shown[4] that sensing material in the nanoparticle phase improves the ratio response/noise (sensitivity) of the chemical sensor. Moreover, it is known that the introduction of small quantities of noble metals (such as palladium or platinum) increases the sensitivity to some gases (i.e. improves selectivity) and the sensor can be operated at lower sensing temperatures (i.e. improving stability).[5−7] Both sensitivity and selectivity also depend on the distribution, chemical state, and cluster size of the added noble metals[5] and, thereby, both mainly depend on the procedure used to obtain the sensing material.[8] Nowadays, impregnation continues to be the most useful addition method.[2,5,9] There are many variations, but the basic procedure consists in the dissolution of a noble metal salt in a proper aqueous solution, stirring this solution together with the base material, and a final drying step. Within this context, the aim of this paper is to present an easy and improved procedure to obtain a tin oxide sensor with added Pd catalyst that also allows us to control its properties, thus avoiding some of the disadvantages shown by existing methods. Electroless metal deposition processes have been widely used since their introduction by Brenner and Riddell[10] to provide metal coating of surfaces by simple immersion in a suitable aqueous solution. Its principles and behavior are well established[11] and, thus, metal deposition is obtained by reduction of metal ions present in the solution by means of a chemical reducing agent. The advantages of the proposed technique are its high reproducibility, mass production potential, time savings, and low cost. Moreover, the reduction of aqueous solutions of Pd(II) salts using a Sn(II) salt is a well-known process of activation of surfaces for further electroless deposition of other catalysts such as Cu[12−14] and Ni.[15] Nevertheless, the Pd(II) electroless process has been scarcely used either for direct palladium addition or for a two-step palladium electroless addition process.[16] In our procedure, SnO_2 nanopowders incorporate palladium catalyst provided from a solution containing $PdCl_2$ and it is deposited via a single-step

* To whom correspondence should be addressed.
† Department of Physical Chemistry.
‡ Department of Electronics.

(1) Seiyama, T.; Kato, A.; Fujisishi, K.; Nagatoni, M. *Anal. Chem.* **1962**, *34*, 1052.
(2) Schweizer-Berberich, M.; Zheng, J. G.; Weimar, U.; Göpel, W.; Bârsan, N.; Pentia, E.; Tomescu, A. *Sens. Act. B* **1996**, *31* (1−2), 71.
(3) Göpel, W. *Sens. Act.* **1989**, *16*, 167.
(4) Xu, Ch.; Tamaki, J.; Miura, N.; Yamazoe, N. *Sens. Act. B* **1991**, *3*, 147.
(5) Yamazoe, N. *Sens. Act. B* **1991**, *5*, 7.
(6) Gaidi, M.; Chenevier, B.; Labeau, M. *Sens. Act. B* **2000**, *62*, 43.
(7) Sauvan, M.; Pijolat, C. *Sens. Act. B* **1999**, *58*, 295.
(8) Lim, C.-B.; Oh, S. *Sens. Act. B* **1996**, *30*, 223.
(9) Sekizawa, K.; Widjaja, H.; Maeda, S.; Ozawa, Y.; Eguchi, K. *Catal. Today* **2000**, *59*, 69.
(10) Brenner, A.; Riddell, G. E. *J. Res. Natl. Bur. Stan.* **1946**, *37*, 31.
(11) Lowenheim, F. A. *Modern Electroplating*; John Wiley & Sons Inc.: New York, 1974.
(12) Shiau, C.-Y.; Tsai, J. C. *J. Chem. Technol. Biotechnol.* **1998**, *73*, 414.
(13) Chang, H.-F.; Yang, C.-F. *Ind. Eng. Chem. Res.* **1997**, *36*, 2080.
(14) Chang, H.-F.; Saleque, M. A.; Hsu, W.-S.; Lin, W.-H. *J. Mol. Catal. A* **1996**, *109*, 249.
(15) Yoshiki, H.; Hashimoto, K.; Fujishima, A. *J. Electrochem. Soc.* **1995**, *142*, 428.
(16) Li, A.; Xiong, G.; Gu, J.; Zheng, L. *J. Membrane Sci.* **1996**, *110*, 257.

10.1021/cm011131h CCC: $20.00
Published on Web 10/17/2001

electroless process with $SnCl_2$ acting as reductor. A set of metal salt and reductor concentrations in the solution are used to analyze the influence on the final catalyst concentration of SnO_2. A set of programmed annealing temperatures is also applied to the samples to know the influence of temperature on the chemical composition of the sample.

Experimental Details

The preparation of catalyzed tin oxide has been typically obtained by adding 2 g of an SnO_2 powder to 100 cm^3 of a $PdCl_2$ aqueous solution with the corresponding palladium concentration in 5×10^{-3} M HCl (since acid enables the palladium salt solution process, we choose the proposed solution to have at anytime an excess of the acid with respect to the different palladium concentrations studied). The solution is then rinsed in a Memmert model WB14 bath provided with a M00 rinsing machine, thus obtaining a solid suspension of the SnO_2 powder in the catalyst solution. The temperature (30 °C) and the rinse rate were maintained during 15 min just to achieve the thermal equilibrium. Then, 10 cm^3 of a freshly prepared aqueous solution of $SnCl_2$ in 5×10^{-3} M HCl is added and the whole solution is rinsed at the same temperature and rate for 50 min.

The basic electroless process is thus as follows:

$$Pd^{2+} + Sn^{2+} \rightarrow Sn^{4+} + Pd \quad E° = 0.800 \text{ V}$$

which can be decomposed into the following half-cell processes:

$$Pd^{2+} + 2e^- \rightarrow Pd \quad \text{(metal reduction)} \qquad E° = 0.951 \text{ V}^{17} \tag{1a}$$

$$Sn^{2+} \rightarrow Sn^{4+} + 2e^- \quad \text{(oxidation)} \qquad E° = -0.151 \text{ V}^{17} \tag{1b}$$

We have used three different nominal atomic Pd/Sn ratios: 0.1, 1, and 5 atom %. These ratios were tried to study the whole range of the usual concentrations used for gas-sensing applications of Pd addition on SnO_2[18] For each Pd/Sn ratio, two different concentrations of $SnCl_2$ in the final solution are used: either stoichiometric concentration Sn^{2+}/Pd^{2+} ratio or 10 times this ratio. Afterward, a filtration using Albet model 420 filters is released, rinsing with diluted HCl and then with water. A final desiccation process at 80 °C was done to collect the final powder.

Then, a thermal treatment is applied on some of the obtained powders using a muffle furnace. This treatment consists of a 8 h heating at the desired temperature (either 200, 450, or 800 °C), reached at a rate of 20 K min^{-1}.

X-ray diffraction (XRD) patterns have been obtained with a Siemens D-500 X-ray diffractometer using Cu Kα radiation (λ = 1.5418 Å), with an operating voltage of 40 kV and a current of 30 mA. Data were collected in steps of 0.05° (2θ) from 20° to 80°.

X-ray photoelectron spectroscopy (XPS) data were collected in a Physical Electronics 5500 spectrometer, working at a vacuum pressure of 8×10^{-7} Pa. Al Kα X-ray source, which produces photons with an energy of 1486.6 eV and a natural line width of 0.9 eV, was used.

A Perkin-Elmer Optima 3200 RL spectrometer was used for the induced coupled plasma-optical emission spectroscopy (ICP−OES) measurements. It has a radio frequency source of 40 MHz, with a working power between 750 and 1500 W and a segmented-array charge coupled device (SCD) detector with simultaneous measure of 235 subarrays.

With respect to the ICP analysis, the knowledge of the analysis process itself is useful for the results presented below. Thus, to analyze the sample, we need to have the sample in solution, and the dissolution process is made in three sequential chemical steps:

(1) The sample is immersed in a solution of aqua regia in order to solubilize all the catalyst species present on the surface. In this process we also solubilize possible tin species not coming from tin oxides. (2) An alkali fusion process with Na_2O_2 and Na_2CO_3 solubilizes tin oxides. (3) If any solid remains after the second step, it is again solubilized in a solution of aqua regia.

A Jobin Yvon T64000 Raman spectrometer with an INNOVA 300 Coherent Ar laser, a triple monochromator (1800 g/mm), a bidimensional charge coupled detector cooled with liquid nitrogen, and an Olympus BH2 microscope was used for Raman analysis.

Transmission electron microscopy (TEM) was carried out on a Phillips CM30 SuperTwin electron microscope operated at 300 keV with 0.19 nm point resolution. For TEM observations, SnO_2 nanopowders were ultrasonically dispersed in ethanol and deposited on amorphous carbon membranes. Image processing was made using DigitalMicrograph and Photoshop software. Lattice spacing values obtained from image processing were compared with those published in JCPDS lists: SnO_2,[19] Pd,[20] and PdO.[21]

All solutions have been prepared with p.a. grade reagents and triply distilled water, which is also used for all water rinses. Products used are $PdCl_2$ (99.9%), $SnCl_2$ (99%), and SnO_2 (99.9%) (all from Alfa) and HCl (37% fuming) from Merck.

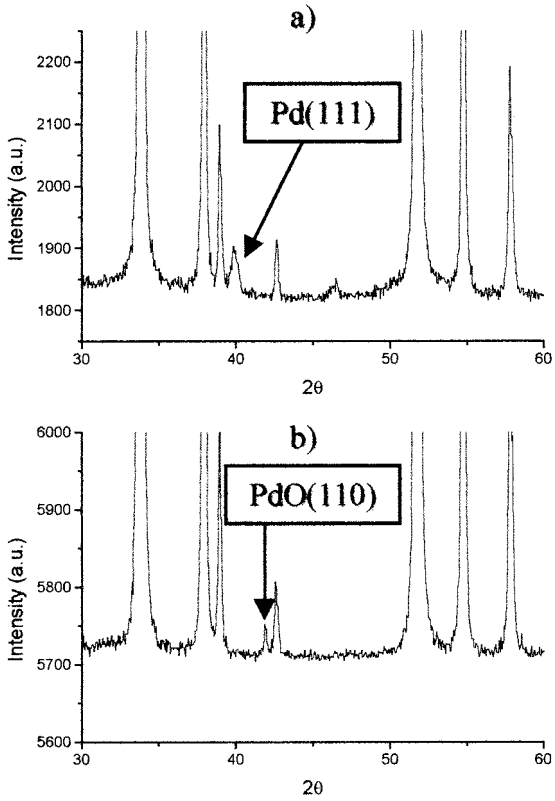

Figure 1. XRD diffractograms of two samples obtained from solutions with nominal 5 atom % Pd and a $SnCl_2$ concentration 10 times the stoichiometric ratio: (a) nonannealed and (b) annealed at 800 °C.

Results and Discussion

The XRD pattern of two samples with the highest catalyst percentage (Figure 1) show the diffractogram obtained for the blank sample (the pattern of this blank

(17) Lide, D. R. *Handbook of Chemistry and Physics*, 78th ed.; CRC Press: New York, 1997.
(18) Matsushima, S.; Tamaki, J.; Miura, N.; Yamazoe, N. *Chem. Lett.* **1989**, 1651.
(19) *JCPDS* **1997**, 41−1445.
(20) *JCPDS* **1997**, 46−1043.
(21) *JCPDS* **1997**, 41−1107.

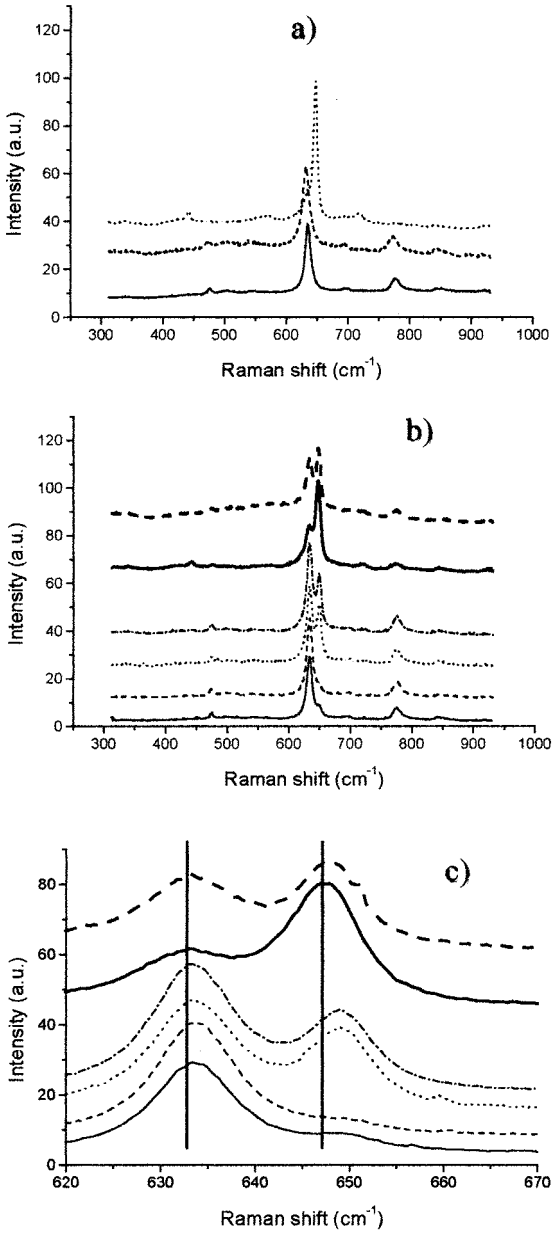

Figure 2. Raman spectra of (a) samples obtained from solutions with nominal 5 atom % Pd and a $SnCl_2$ concentration 10 times the stoichiometric ratio: −, nonannealed; ---, annealed at 200 °C; ▪▪ annealed at 800 °C. Raman spectra of (b) samples annealed at 450 °C: −, nominal 0.1 atom % Pd, stoichiometric $SnCl_2$; ---, nominal 0.1 atom % Pd, a $SnCl_2$ concentration 10 times the stoichiometric ratio; ▪▪, nominal 1 atom % Pd, stoichiometric $SnCl_2$; −·−, nominal 1 atom % Pd, a $SnCl_2$ concentration 10 times the stoichiometric ratio; **—** nominal 5 atom % Pd, stoichiometric $SnCl_2$; −−, nominal 5 atom % Pd, a $SnCl_2$ concentration 10 times the stoichiometric ratio. (c) A close up view of spectra (b.)

sample is that of cassiterite[19]) with some additional phases corresponding to the added catalyst. The mean grain size calculated from the Debye−Scherrer equation for the used SnO_2 is of 62 ± 2 nm for the nonannealed samples. This size increases slightly with the annealing temperature, reaching a mean grain size of 65 ± 1 nm in the samples annealed at 800 °C. With respect to the added catalyst, in the nonannealed sample only the peaks corresponding to metallic palladium are detected (Figure 1a)[20] and in the one annealed at 800 °C only those of PdO are present (Figure 1b).[21] The evidence of

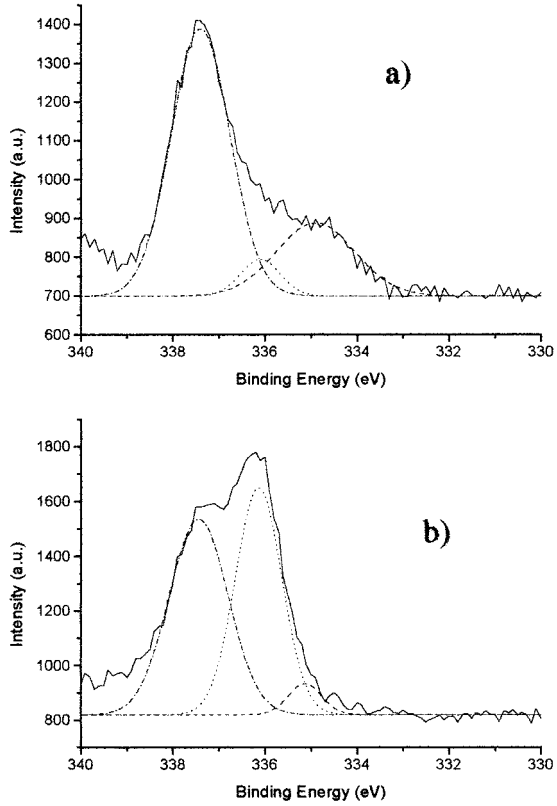

Figure 3. XPS spectra of the samples obtained from solutions with nominal 5 atom % Pd and a $SnCl_2$ concentration 10 times the stoichiometric ratio: (a) nonannealed; −, acquired spectrum; ---, metallic palladium; ▪▪, PdO; −·−, $PdCl_2$; (b) annealed at 800 °C; −, acquired spectrum; ---, metallic palladium, ▪▪, PdO; −·−, PdO_2.

PdO after annealing at sufficiently high temperature is in agreement with the results reported for samples obtained by using other addition techniques.[22−24] In the samples with lower nominal catalyst concentrations, no XRD palladium phases have been detected, because the abundance of these phases lies below the XRD detection limit, but the same behavior is expected, as we will show below.

Raman spectra of the whole set of samples (Figure 2) show that among all the possible SnO_2 Raman bands[25,26] we studied those bands currently detected, i.e., A_{1g} (630 cm^{-1}), B_{2g} (774 cm^{-1}), and E_{1g} (472 cm^{-1}).[27] In the added catalyst samples, no additional Raman band is detected in the nonannealed samples. This means that the main part of the palladium in these samples is present in the metallic state because of the high reflectivity of metals to the laser radiation used in Raman measurements. The presence of other palladium states (like $PdCl_2$) at sufficiently high concentration would have shown additional Raman bands. An additional Raman band at 650 cm^{-1} is obtained when the sample is annealed either at 450 or 800 °C, which is attributed to the most intense

(22) Rella, R.; Serra, A.; Siciliano, P.; Vasanelli, L.; De, G.; Licciulli, A. *Thin Solid Films* **1997**, *304*, 339.
(23) Egashira, M.; Nanashima, M.; Kawsumi, S. *ACS Symp. Ser.* **1986**, *309*, 71.
(24) Su, S. C.; Carstens, J. N.; Bell, A. T. *J. Catal.* **1998**, *176*, 125.
(25) Scott, J. F. *J. Chem. Phys.* **1970**, *53*, 852.
(26) Katiyar, R. S.; Dawson, P.; Hargreave, M. M.; Wilkinson, G. R. *J. Phys. C* **1971**, *4*, 2421.
(27) Yu, K. N.; Xiong, Y.; Liu, Y.; Xiong, C. *Phys. Rev. B* **1997**, *55*, 2666.

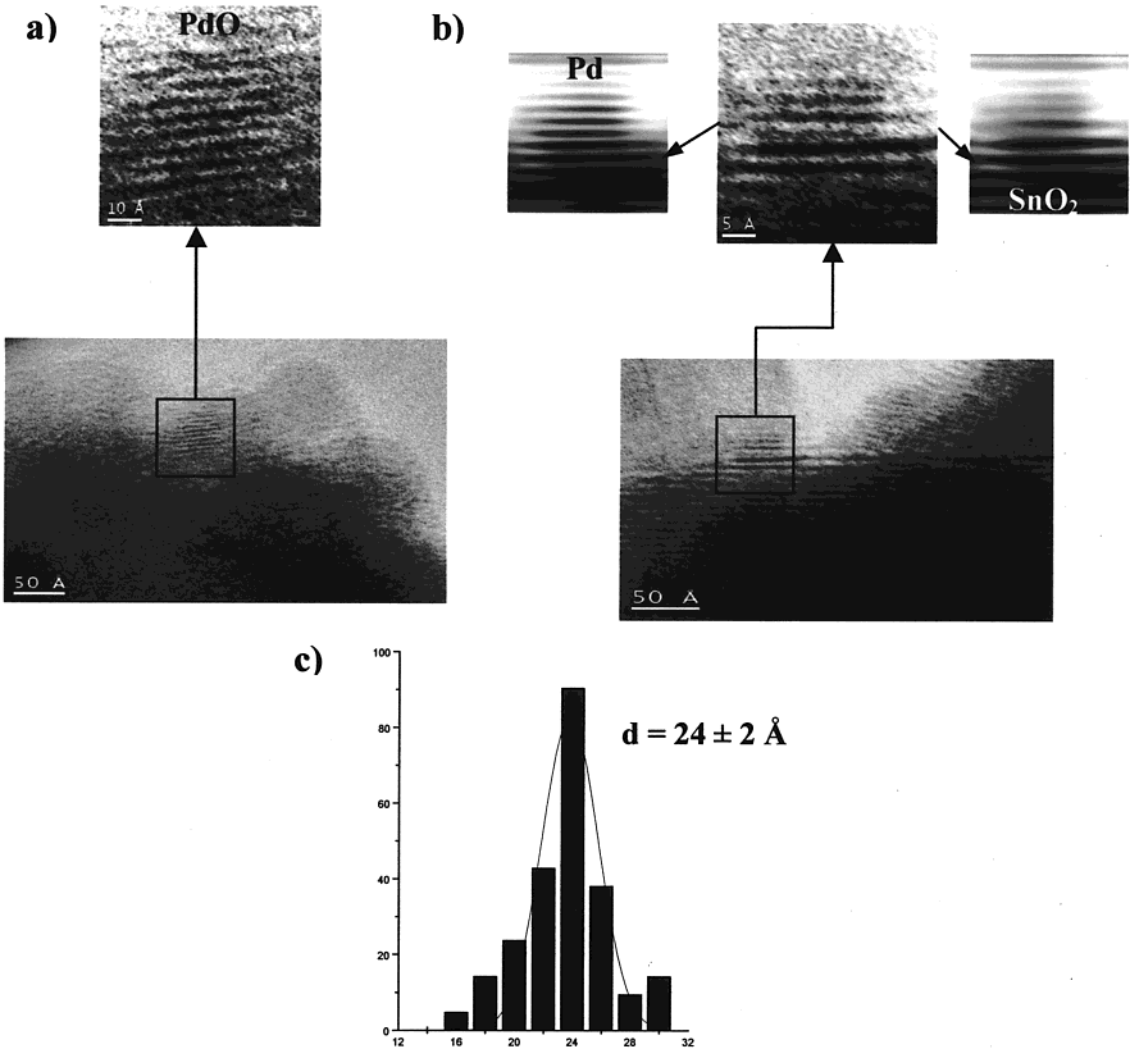

Figure 4. HRTEM images showing Pd and PdO phases in the sample with nominal 5 atom % Pd and a $SnCl_2$ concentration 10 times the stoichiometric ratio annealed at 800 °C. (a) PdO nanocluster embedded on a SnO_2 nanoparticle's surface. (b) A Pd nanocluster on a SnO_2 surface. The filtered images separating Pd and SnO_2 planes are also shown. (c) Mean diameter size histogram of PdO nanoclusters measured on several HRTEM images.

and practically the unique visible PdO Raman band.[24] The area ratio of this band with respect to that of SnO_2 A_{1g} Raman band increases with catalyst concentration (Figure 2b). The two other SnO_2 Raman bands decrease their area as the catalyst concentration increases until they disappear, and as a result, the SnO_2 Raman spectra is completely masked (Figure 2a). In addition, the PdO and the SnO_2 A_{1g} Raman bands shift to more negative values as the catalyst concentration increases (Figure 2c). All shifts were corrected taking as reference the silicon Raman band at 520 cm^{-1}. The shift in Figure 2c allows us to speculate about the possible incorporation of palladium in to the SnO_2 structure.

To know where the catalyst is distributed in the SnO_2 nanopowders, we have also investigated the XPS response of the set of prepared samples. The spectra of the sample with the highest catalyst concentration without annealing and after annealing at 800 °C are shown in parts a and b of Figure 3, respectively. All the spectra were fitted to reach the right carbon position (284.5 eV).[28] Fittings are performed considering 80/20% Gaussian/Lorentzian orbital peaks and Shirley baselines,[29] and the fitting results verify the presence of both metallic palladium ($3d_{5/2}$ peak at 335.1 eV)[30] and Pd-(II) at any annealing temperature. Pd(II) is mainly present as the chloride ($3d_{5/2}$ peak at 337.2 eV)[31] at low annealing temperatures and as PdO ($3d_{5/2}$ peak at 336.1 eV)[32] after annealing at 800 °C, where no chlorides were detected. At high annealing temperatures there is the additional presence of a higher oxidation state of Pd, i.e., PdO_2 ($3d_{5/2}$ peak at 337.6 eV),[33] that has not been detected in the bulk.

Figure 4 shows the TEM analysis of the sample with the highest catalyst concentration annealed at 800 °C. A mixture of metallic Pd and PdO on the surface of the SnO_2 nanopowders is observed, and palladium was demonstrated to be placed on the SnO_2 surface, forming metallic Pd and PdO nanoclusters. Figure 4a enlights

(28) Chastain, J. *Handbook of X-ray Photoelectron Spectroscopy*; Perkin-Elmer Corp.: Minnesota, 1992.

(29) Shirley, D. A. *Phys. Rev. B* **1972**, *5*, 4709.
(30) Nyholm, R.; Martensson, N. *J. Phys. C* **1980**, *13*, L279.
(31) Kumar, G.; Blackburn, J. R.; Albridge, R. G.; Moddeman, W. E.; Jones, M. M. *Inorg. Chem.* **1972**, *11*, 296.
(32) Kim, K. S.; Gossman, A. F.; Winograd, N. *Anal. Chem.* **1974**, *46*, 197.
(33) Phani, A. R.; Manorama, S.; Rao, V. J, *J. Phys. Chem. Sol.* **2000**, *61*, 985.

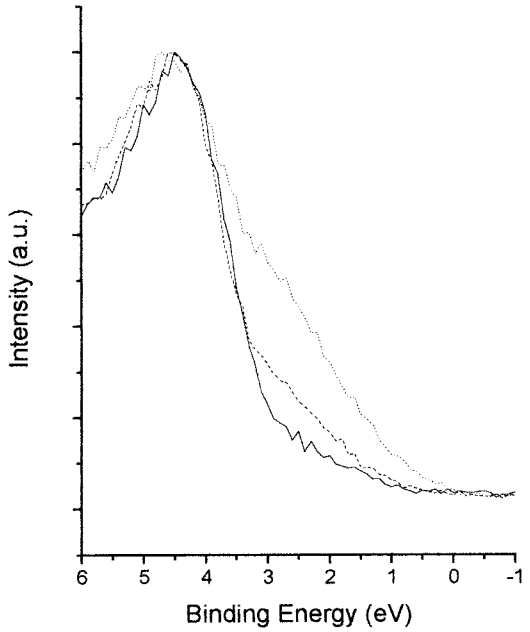

Figure 5. VB spectra for samples with a $SnCl_2$ concentration 10 times the stoichiometric ratio annealed at 800 °C: —, nominal 0.1 atom % Pd; ---, nominal 1 atom % Pd; and ···, nominal 5 atom % Pd.

a PdO nanocluster placed on the surface of a SnO_2 nanoparticle. The lattice spacing of the nanocluster was calculated by the fast Fourier transform (FFT) of the TEM micrograph. In this case, we obtained 2.15 Å, corresponding to the (110) PdO planes. In Figure 4b a Pd nanocluster was imaged also on the SnO_2 nanoparticle surface. We applied several frequency filters on the FFT image in order to separate those planes corresponding to Pd from those corresponding to SnO_2 planes. Lattice spacing were also calculated on FFT space and we obtained 3.35 Å in the case of SnO_2, corresponding to (110) planes, and 2.25 Å in the case of Pd, corresponding to $(1\bar{1}1)$ planes.

The density of Pd nanoclusters on the SnO_2 grain surface has been measured from the TEM images, yielding $(2.2 \pm 0.2) \times 10^{12}$ cm^{-2}. Measurements performed on different SnO_2 particles have shown the homogeneous distribution of these nanoclusters. After analyzing over 100 nanoclusters we have found that approximately 90% of them are oxidized (PdO), while just 10% remain metallic (Pd). The mean diameter size obtained for these nanoclusters is 24 ± 2 Å (see Figure 4c). Following these results, we can conclude that the electroless method allowed us to obtain better nanocluster dispersion in the case of Pd than those impregnation methods reported before elsewhere.[34,35] As shown in previous contributions,[34,35] in the case of Pd loaded on SnO_2 nanopowders using impregnation methods, hardly any nanocluster formation was found on the semiconductor's surface.

The valence band of the samples after annealing at 800 °C obtained by XPS is shown in Figure 5. Surface states at the top of the valence band, below the Fermi level, are observed and, as previously reported,[36] can be associated with the catalyst. The density of states increases, of course, with catalyst concentration.

Table 1. ICP Results of the Samples with the Highest Catalytic Percentage

nominal Pd/Sn (atom %)	nominal $SnCl_2/PdCl_2$	annealing temp (°C)	Pd found/ nominal Pd (%)	$SnCl_2$ (atom %)	Pd inserted/ total Pd (%)
5	1		45	0.013	0
5	1	800	34.4	7×10^{-4}	71.95
5	10		87	0.069	0
5	10	800	48	0.003	80

With respect to the ICP results, they are summarized in Table 1. Only a few ICP partial results are reported for impregnated samples.[37] In our case, the results show that the efficiency of the electroless method for the catalyst addition to the SnO_2 nanopowders is very high, specially when using a higher reductor concentration, where we can find almost 90% of the expected Pd, although in these samples the percentage of species coming from the reductor salt present on the SnO_2 surface is also higher if no annealing was applied. Nevertheless, it should be stated that the chemical process described here is not able to distinguish between different oxidation states or compounds of palladium and, thus, we are referring to total palladium (i.e., the total palladium quantity coming from either metallic Pd, $PdCl_2$, PdO or any other palladium compound). This efficiency has the same average value as that obtained in classical impregnation and much higher than that of impregnation without evaporation to dryness.[38] The efficiency decreases for annealed samples mainly due to the loss of catalyst during the heating process and also to the conversion of the reductor species, tin cations, to tin oxide, because almost no reductor species are detected after annealing. Moreover, the ICP results showed that, in annealed samples at 800 °C, most of the palladium is dissolved in the third chemical step described in the Experimental Section. It could be possible that palladium would be insoluble in aqua regia for a determined palladium compound, but although, for example, Pd−Sn alloys have been previously reported,[39] no evidence neither of these alloys nor of mixed oxides have been obtained by us, so the most suitable interpretation is that almost all the palladium dissolved in the third chemical step is inside the SnO_2. This interpretation will also explain the Raman spectra modifications yet described.

Acknowledgment. The autors would like to thank Tomás Muriel, Josep Lluis Alay, Tariq Jawhari, and Elionor Pelfort from the XRD, XPS, Raman, and ICP units of the Serveis Cientifico Tecnics of the University of Barcelona for their work. This work has been partially funded by project 2FD97-1804.

CM011131H

(34) Diéguez, A.; Vilà, A.; Cabot, A.; Romano-Rodríguez, A.; Morante, J. R.; Kappler, J.; Bârsan, N.; Weimar U.; Göpel, W. *Sens. Act. B* **2000**, *68*, 94.
(35) Cabot, A.; Arbiol, J.; Morante, J. R.; Weimar, U.; Bârsan N.; Göpel, W. *Sens. Act. B* **2000**, *70*, 87.
(36) Diéguez, A. Ph.D. Thesis; University of Barcelona, Barcelona, 1999.
(37) Laurein, W.; Delabie, L.; Huyberechts, G.; Maes, G.; Roggen, J.; Stevens, G.; Vinckier, C. *Sens. Act. B* **2000**, *65*, 193.
(38) Unpublished results.
(39) Mathon, M.; Gambino, M.; Hayer, E.; Gaune-Escard, M.; Bros, J. P. *J. Alloys Compd.* **1999**, *285*, 123.